02B-50

# Triangulation Position Error Analysis for Closely Spaced Imagers

**John N. Sanders-Reed**
Boeing-SVS, Inc.



## ABSTRACT

This paper provides an error analysis for a typical two camera, 3D triangulation system used in automotive crash test analysis. Accuracy of this 3D measurement for analysis of simple planar motion is compared to the accuracy expected from a comparable single sensor analysis system using calibration objects within the field of view. Both approaches are shown to produce errors on the order of 1 mm, object to object or frame to frame. This work also demonstrates how to utilize basic triangulation error equations to start from a given accuracy requirement and flow down an error budget in order to develop the basic sensor geometry and measurement requirements. The current work extends previous theoretical work which developed the basic error propagation theory for 3D triangulation.

## 1. INTRODUCTION

Automotive crash test facilities use high speed imaging sensors (cameras) to generate image sequences for quantitative motion analysis. The motion analysis is intended to determine position versus time, and hence velocity and acceleration versus time, of vehicle occupants during various crash scenarios. Traditionally, single camera solutions have been the norm, resulting in the analysis of planar motion. Recently, interest has developed in the use of multiple imaging sensors to provide triangulation capability to compute three dimensional positions. The first published work on this topic in the automotive field was by Walton [1]. Parallel work in the defense community was performed by Sanders-Reed [2]. While these efforts resulted in a 3D position estimation capability, the accuracy of results was difficult to predict. Recent work by Sanders-Reed [3] has provided an analytical framework with which to analyze specific experimental configurations. Other applications of multi-sensor triangulation include particle flow velocimetry and analysis [4,5]. The current paper simplifies and uses the results of [3] to evaluate the accuracy associated with typical 2 camera, crash test scenarios and conversely describes the process of designing a test setup to achieve a specified level of accuracy.

We will address two problems in this paper. The first and simpler problem is to estimate the 3D position accuracy which can be obtained from a given test setup. In this case, the test geometry, camera parameters, and measurement errors are given, and we desire to determine the accuracy of our 3D position measurement. This problem also allows us to compare the accuracy obtained from a 2 camera triangulation system, with that obtained using a more traditional, single camera system and assuming planar motion. The second problem begins with a stated 3D position measurement accuracy requirement. From that requirement, we flow down an error budget to the various contributing measurements and the geometric setup, in order to design a test which meets the accuracy requirement. However, in order to tackle these two problems, we need first to simplify the results obtained in reference [3].

We begin, in section 2, by re-writing the key results from reference [3] in order to highlight the functional form of the results. We extend the previous work by generating more generalized plots of the coefficients which lend themselves to more practical application. Section 3 describes how to determine the 3D position accuracy resulting from a given test setup, while section 4 describes how to flow down an error budget in order to meet a given accuracy requirement.

## 2. TWO-SENSOR ERROR ANALYSIS

Accuracy of 3D position estimates of a target, using multi-sensor triangulation techniques, is determined by the accuracy of sensor location and sensor to target Line Of Sight (LOS) knowledge, and the geometry of the measurement system. For each sensor, we need to know the 3, sensor location parameters (x,y,z), and the LOS vector (azimuth, $\theta$ and elevation, $\varphi$) from the sensor to the target (Figure 1). This is obvious from the 3D triangulation equations (1)-(4) (equations (6), (7), (3), (2) from reference [3]), in which the subscripts 1 and 2 refer to sensors 1 and 2.

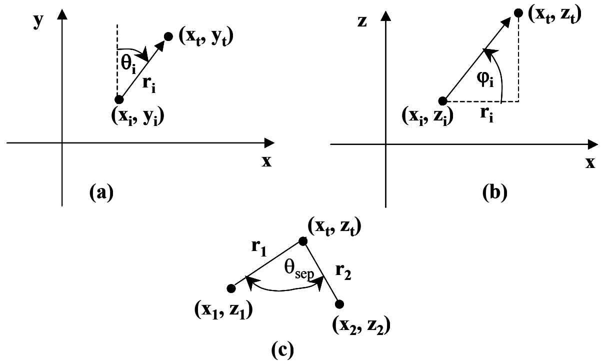


Figure 1. Definition of coordinate system showing target location ($x_t$, $y_t$, $z_t$) and sensor location ($x_i$, $y_i$, $z_i$): a) x-y plane view showing azimuth angle and horizontal range, b) x-z plane view showing elevation angle, c) x-y plane showing sensor to sensor separation angle.

$$x_t = \frac{\left[x_2 \tan\theta_1 - x_1 \tan\theta_2 + (y_1 - y_2)\tan\theta_1 \tan\theta_2\right]}{\left(\tan\theta_1 - \tan\theta_2\right)} \quad (1)$$

$$y_t = \left[y_1 \tan\theta_1 - y_2 \tan\theta_2 + x_2 - x_1\right]\left(\tan\theta_1 - \tan\theta_2\right)^{-1} \quad (2)$$

$$r_i = \sqrt{(x_i - x_t)^2 + (y_i - y_t)^2} \quad (3)$$

$$z_t = r_i \tan\varphi_i + z_i \quad (4)$$

These five parameters themselves may each depend on several other measurements, each of which has an error component (Figure 2). For example, knowledge of the LOS to the target depends on both knowledge of the LOS of the sensor (which may not be pointed directly at the target), knowledge of the target location within the image, and the relation between these two parameters. Note that Figure 2 is not comprehensive and in fact, various different measurement parameters will be introduced depending on whether the sensors are on fixed tripods or tracking mounts, whether the sensor is on a moving platform or a fixed pedestal. For the applications described in this paper, we assume that the cameras are mounted on fixed tripods such that the sensor location, and the sensor boresight pointing remain fixed during a given test. This leaves the target location within the imagery as the only dynamic measurement which changes over time.

In order to relate measurement errors to errors in our final position estimates, we begin by assuming that measurement errors obey gaussian statistics. We also assume that measurement errors are independent for each sensor, and that the standard deviation of sensor location measurements is the same in each axis. Next we define some notation: The standard deviation of sensor position measurements is $\sigma_{pos}$, the standard deviation of azimuth measurements as $\sigma_\theta$, and the standard deviation of elevation measurements as $\sigma_\varphi$. We can compute the horizontal sensor to target range, r for each sensor. The standard deviation of this result will be $\sigma_r$. We will compute the target location ($x_t$,$y_t$,$z_t$). Each of these values with have an associated error value: $\sigma_{xt}$, $\sigma_{yt}$, $\sigma_{zt}$.

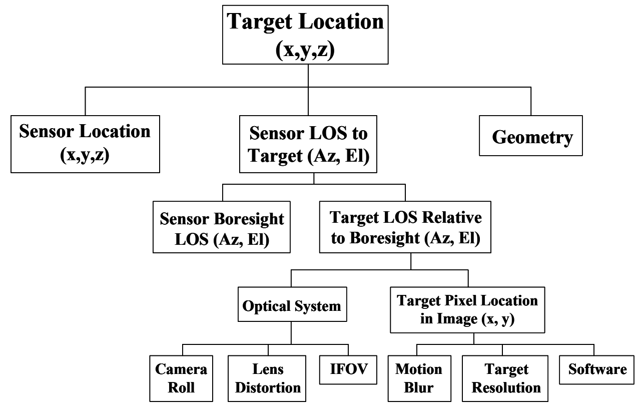


Figure 2. Typical contributing error sources for 3D position estimation

The preceding assumptions lead to the key results of reference [3]: the error propagation equations (22), (23), (24), and (20), which relate the measurement errors to computed values of $x_t$, $y_t$, r, $z_t$, respectively. These equations include detailed formulae for computation of the coefficients of the error terms as complex sums of various partial derivatives. In order to show the basic functional form of the error propagation equations, and to support tabulating values for the coefficients, the reference [3] equations have been re-written with the coefficients as simple scalar constants in equations (5)-(8):

$$\sigma_{x_t} = \sqrt{c_{x,pos}^2 \sigma_{pos}^2 + (rc_{x,\theta})^2 \sigma_\theta^2} \quad (5)$$

$$\sigma_{y_t} = \sqrt{c_{y,pos}^2 \sigma_{pos}^2 + (rc_{y,\theta})^2 \sigma_\theta^2} \quad (6)$$

$$\sigma_{r_i} = \sqrt{c_{r,pos}^2 \sigma_{pos}^2 + (rc_{r,\theta})^2 \sigma_\theta^2} \quad (7)$$

$$\sigma_{z_t} = \sqrt{c_{z,r}^2 \sigma_r^2 + (rc_{z,\varphi})^2 \sigma_\varphi^2 + \sigma_{pos}^2} \quad (8)$$

The error coefficients are functions of the sensor-to-sensor separation angle (Figure 1). The coefficients of the LOS errors are also linear functions of the sensor to target range, as indicated by writing them as *(rc)*. Reference [3] contains graphs of the values of the coefficients as a function of the sensor-to-sensor separation angle, however those graphs must be used with care. The graphs are of the *c* and *(rc)* values in the equations above, but it is not clear in that paper whether the graphs are of *c*, *(rc)*, or of $c^2$, $(rc)^2$. Reference [3] also indicates that the coefficient values in the graphs were computed for a sensor to target range of 5 units, and that the coefficients of the LOS errors must be scaled linearly with range. Equations (5)-(8) are written to make this scaling factor explicit, visible, and separate from the *c* values.

The position and azimuth coefficients for the x and y position error exhibit some dependence not only on the sensor-to-sensor separation angle, but also on the absolute azimuth angle. This is a rather artificial effect which can be altered by choice of the origin and the zero azimuth direction. While this effect may seem strange, one should note that any decrease in error in the x position is offset by a corresponding increase in the error in the y direction. In fact, this effect disappears when measuring the sensor to target range error, since this calculation requires both x and y target position estimates.

The graphs in reference [3] show multiple curves for each coefficient (for the x and y position error), depending on the absolute orientation of the sensor pair relative to the coordinate axes. A more useful graph for most practical applications, would average the curves for the different absolute orientations. When this is done, one finds that $c_{x,pos} = c_{y,pos}$ and $c_{x,\theta} = c_{y,\theta}$. Performing this averaging and factoring out the range dependence as shown in equations (5)-(8), gives the graphs shown in Figure 3 for the coefficients in equations (5), (6).

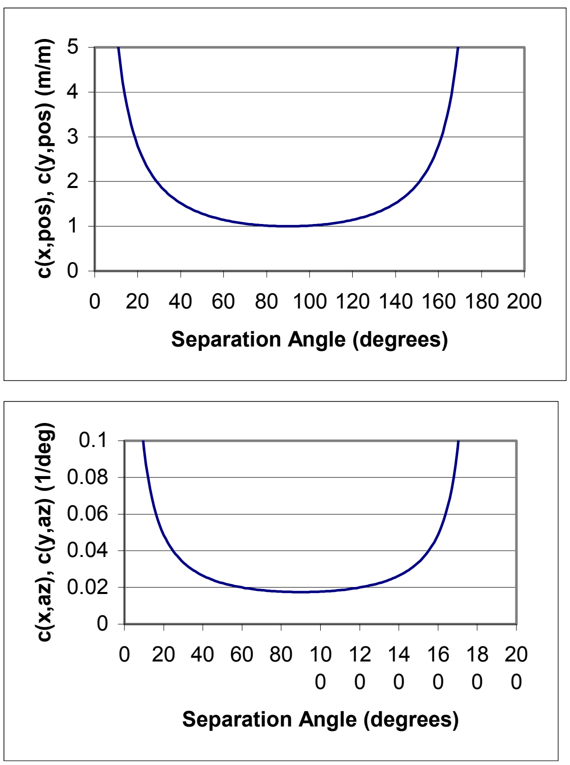


Figure 3. Error propagation coefficients for equations (5), (6), relating sensor location errors in meters and LOS errors in degrees to target (x,y) location estimate errors in meters.

As already discussed, the sensor to target horizontal range estimates are independent of absolute sensor positioning relative to the coordinate system, so the averaging performed to generate the curves in Figure 3 is not necessary. Figure 4 shows curves for the range coefficients in equation (7). Figure 5 shows plots for the target z position error coefficients from equation (8).

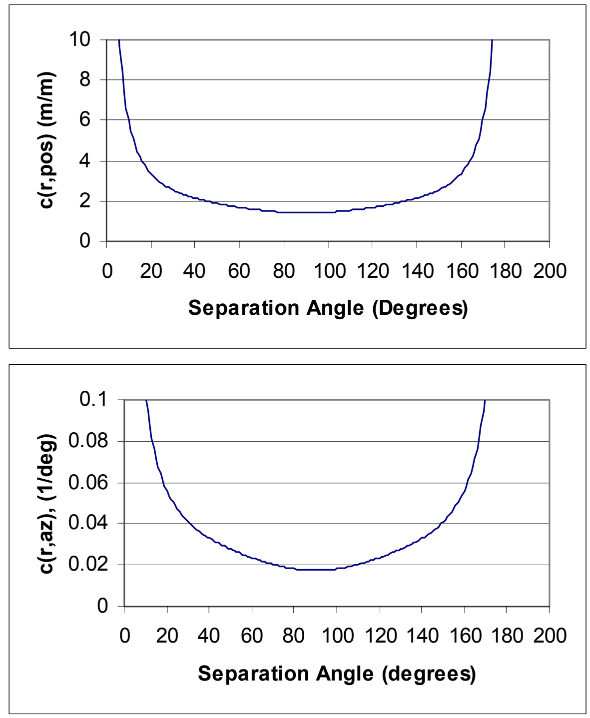


Figure 4. Error propagation coefficient for equation (7) relating sensor location errors in meters and LOS errors in degrees to sensor to target horizontal range estimate errors in meters.

These graphs emphasize the well known fact that the geometry least sensitive to measurement errors places the cameras at a 90 degree separation angle with a 0 degree elevation angle. The error coefficients do not begin to grow rapidly until the separation angle decreases to less than 40 degrees.

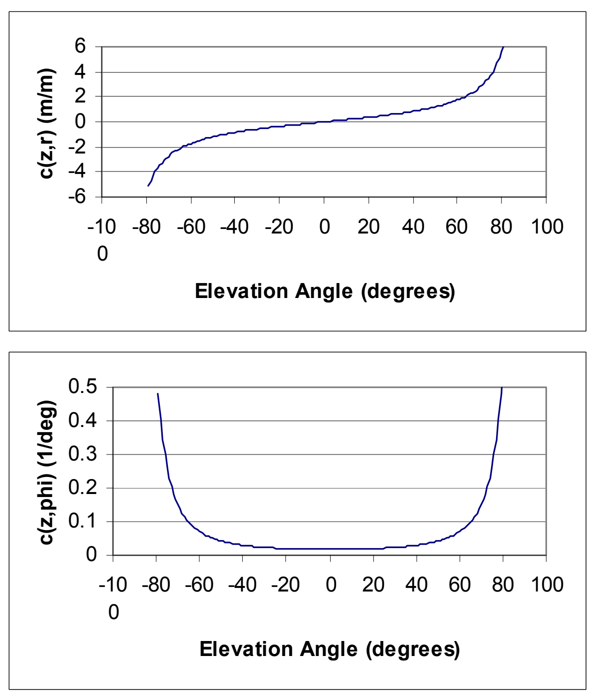


*Figure 5. Error propagation coefficient for equation (8), relating sensor location errors in meters and LOS errors in degrees to target z position estimate errors in meters.*

In the following sections we will read error coefficient values off of these graphs and use them in equations (5)-(8) in order to generate error estimates.

## 3. EVALUATION OF RANGE ACCURACY

In many test scenarios, most of the parameters are fixed and the best that we can do is evaluate the accuracy of our 3D position estimates. The geometry may be dictated by viewing requirements: camera-to-camera baseline may be constrained by spacing considerations or Line Of Sight (LOS) limitations, while sensor to target range is constrained by the need to cover the Field Of View (FOV) of motion. Camera parameters, such as pixel count, are determined by currently available cameras and limited by state-of-the-art in technology, or acquisition cost.

In this section we will define a typical automotive crash test geometry and camera parameters, assign an achievable accuracy limit to various parameters, such as sensor location and LOS pointing, and target track accuracy. From this we will determine the accuracy of our 3D position estimates.

We will examine the accuracy of both absolute 3D position measurement and relative position measurement. Relative position measurement is by far the most common scenario, in which one wishes to measure the position of one object relative to another in the same test sequence using the same sensors (cameras). This is the case when measuring the position of a dummy relative to a portion of the vehicle. Absolute position measurement is necessary when comparing the position of an object as measured by two different sensor systems, such as a camera system and a radar system or an on-board Inertial Navigation Unit (INU).

Perhaps the most important relative position estimate is the measurement of a single target in each of a series of image frames. The difference in position is the velocity of the target. This means that any measurement errors that cancel out in this measurement will not affect the fundamental quantities of velocity and acceleration.

We will use the test setup shown in Figure 6, in which the cameras are located 2.5 m from the plane of motion with a 2 m Field Of View (FOV) perpendicular to the LOS where the LOS intercepts the plane of motion. In order to provide a view into the vehicle unobstructed by door supports, the cameras are constrained to a 1.5 m baseline. The cameras are located at the same vertical height as the target. We assume 1000x1000 pixel cameras as this represents the state of the art in high speed digital electronic cameras and is comparable to the resolution achievable with 16 mm film. The test setup uses a laboratory defined Cartesian coordinate system.

We define a right handed coordinate system with the origin at the point of intersection of the LOS of the cameras, such that positive x increases horizontally to the right, positive z increases upward (out of the paper), and positive y increases as shown. The cameras are then located at positions (-0.75, -2.5, 0) and (0.75, -2.5, 0).

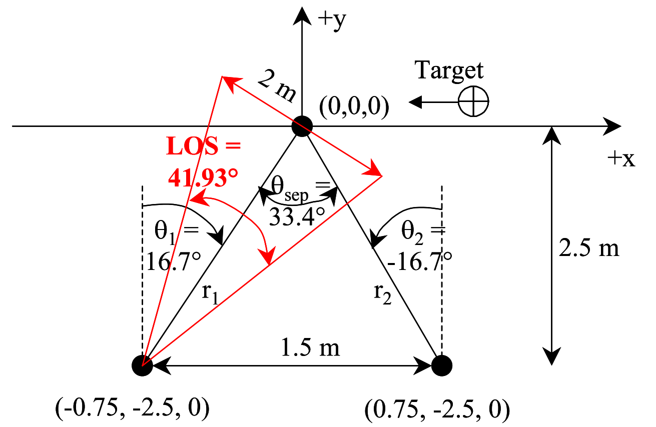


Figure 6. Test setup showing camera locations, separation angle, FOV.

We assume that we can measure camera locations to within $\sigma_{pos}$ = 3 mm (either directly or through calibration) and LOS to within 1 pixel. We further assume that geometric lens distortion inherent in wide-angle lenses can be removed during post-processing of the image data, and that a track accuracy of 0.5 pixels can be achieved. The total LOS error is the quadrature sum of the sensor LOS and the target position error, or $\sigma_\theta = \sigma_\varphi = \sqrt{1^2 + 0.5^2}$ = 1.1 pixels. Note that the track accuracy measurement is the only parameter whose value will change throughout the experiment, and that all of the other measurements errors described here (camera location and LOS) are static (of course this statement only applies to the described setup, other applications, for example using tracking mounts, will have more dynamic parameters).

With this simple description we will quickly compute values for the camera-target-camera separation angle, the camera pointing angles, the angular FOV, and the Incremental Field Of View (IFOV) of a single pixel. Armed with this information we can readily apply the results of section 2 to obtain estimates of the 3D position accuracy. The cameras will have a separation angle of 33.4 degrees, a range to the origin of 2.6 m, azimuth pointing of 16.7 and –16.7 degrees (both with an elevation angle of 0 degrees), a horizontal FOV of 41.93 degrees, and an IFOV of 732 micro-radians. This allows us to convert the LOS error from pixel units to angular units: $\sigma_\theta = \sigma_\varphi$ = 805 micro-radians = 0.046 degrees.

The next task is to determine the error coefficients in equations (5)-(8), from the graphs in section 2. For each of the first 6 coefficients, we refer to the appropriate graph in Figure 3 and 4 and read off the value for a sensor-to-sensor separation angle of 33 degrees. For the last two (z position coefficients) we refer to the graphs in Figure 5 and read off the value for a 0 degree elevation angle. The results are shown in Table 1.

**Table 1. Measurement error coefficients for 33 degree sensor separation**

| **Coef.** | c(x,pos) | c(y,pos) | c(x,LOS) | c(y,LOS) | c(r,pos) | c(r,LOS) | c(z, LOS) | c(z,r) |
|---|---|---|---|---|---|---|---|---|
| **Value** | 1.778 | 1.778 | 0.031 | 0.031 | 2.403 | 0.038 | 0.017 | 0 |

Inserting these values into equations (5)-(8), along with the horizontal sensor to target range of 2.6 m and our measurement error values of $\sigma_{pos}$ = 0.003 m and $\sigma_\theta = \sigma_\varphi$ = 0.046°, we obtain estimates of our target position error. In table 2, we show the error contribution for position measurement error, LOS measurement error, and the total measurement error. Overall, we are seeing about 6 mm accuracy (with slightly more coming from sensor position error than from sensor to target LOS error) in our target position estimates (4 mm in z). Recall that this is for 33° separation and a 2.6 m sensor to target range.

**Table 2. Target position error estimates for 33 degree sensor separation**

| Target parameter | Error (m) from position error $\sigma_{pos}$ | Error (m) from LOS error, $\sigma_{LOS}$ | Total error(m) |
|---|---|---|---|
| $x_t$ | 0.0053 | 0.0037 | 0.0065 |
| $y_t$ | 0.0053 | 0.0037 | 0.0065 |
| r | 0.0072 | 0.0046 | 0.0085 |
| $z_t$ | 0.003 | 0.0020 | 0.0036 |

It is interesting to inquire how much of this error represents a constant bias error for the experiment, and how much is dynamic within the experiment. The only dynamic measurement is the target location measurement within the image. Recall that we estimated a 0.5 pixel estimation accuracy for the target location. This corresponds to a 366 micro-radian accuracy or 0.021 degrees. From equations (5)-(8), we can estimate the track error contribution as shown in table 3. We see our ½ pixel tracking accuracy gives about 2 mm frame-to-frame accuracy for this test setup.

**Table 3. Position error (m) from tracking error for 33 degree sensor separation**

| **xt** | **yt** | **r** | **zt** |
|---|---|---|---|
| 0.0017 | 0.0017 | 0.0021 | 0.0009 |

It is interesting to compare this with a single sensor, 2D calibration measurement. Using a single sensor, one assumes that all motion is in a plane, and that one has a known calibration object in the plane of the motion. One then measures the distance in pixels between two points on the calibration object, and obtains an estimate of the conversion from pixels to meters (or whatever linear units are being used). In our case, we know we have a 2 m FOV with 1000 pixels across, so we have 2 mm per pixel. With a ½ pixel tracking accuracy, this method will yield a 1 mm frame to frame tracking accuracy. Of course, if the reference object is not in the plane of the target motion, the calibration will be off and the actual results will be worse than predicted here.

If we consider ways to improve the accuracy of our measurement, we need to consider whether we need to improve the absolute position measurement, or only the object to object and frame-to-frame position accuracy. Since the target position error due to sensor location error is about equal to the error due to LOS error, if we are concerned with absolute position accuracy, we need to concentrate equally on both. If we are only concerned with object to object and frame-to-frame tracking accuracy, then we need only concentrate on the LOS error related to tracking error. In either case, the easiest thing we can consider is to increase the sensor to sensor separation angle toward 90 degrees. This will have the effect of reducing all of the error coefficients.

Since the error related to sensor position measurements does not depend on sensor to target range, the only other thing which can be done to reduce this term is to improve the sensor location measurement, i.e. reduce $\sigma_{pos}$.

In order to reduce contributions due to LOS error, we can seek to reduce our measurement error. Improvement in our absolute sensor pointing knowledge will reduce our absolute position errors, while improvement in our tracking accuracy will reduce both our absolute errors and our target to target or frame-to-frame errors. Reduction of these errors can be accomplished either by improving the basic measurement (sensor pointing to better than 1 pixel, tracking to better than ½ pixel), or we could attempt to reduce the IFOV. However that involves either adding more pixels within the FOV (i.e a higher resolution camera), or reducing the FOV, which may not be possible due to experimental constraints. Of course both improved tracking accuracy or reduced IFOV could equally well be applied to a 2D scaling approach. Reducing the sensor to target range will reduce the range factor in the LOS error term in equations (5)-(8), however, assuming that we have to increase the angular FOV in order to maintain our 2 m coverage, this will increase the IFOV by an approximately equal factor, resulting in no net change.

Since increasing the sensor-to-sensor separation angle is the easiest thing which can be done to reduce the effect of measurement errors, it is worth asking how much we can reduce our errors by increasing the separation from 33 to 90 degrees. The error coefficients for a 90 degree separation are given in table 4. Examining only the ½ pixel tracking error given in table 5, we find that our object to object or frame-to-frame error has been reduced to about 1 mm.

**Table 4. Measurement error coefficients for 90 degree sensor separation**

| Coef. | c(x,pos) | c(y,pos) | c(x,LOS) | c(y,LOS) | c(r,pos) | c(r,LOS) | c(z, LOS) | c(z,r) |
|---|---|---|---|---|---|---|---|---|
| Value | 1 | 1 | 0.017 | 0.017 | 1.414 | 0.017 | 0.017 | 0 |

**Table 5. Position error (m) from tracking error for 90 degree sensor separation**

| xt | yt | r | zt |
|---|---|---|---|
| 0.0009 | 0.0009 | 0.0009 | 0.0009 |

## 4. FROM ACCURACY REQUIREMENTS TO TEST SETUP

In this section we begin with a requirement to obtain 1 mm frame to frame track accuracy and an overall 5 mm absolute position accuracy. We are constrained by technology to a 1000x1000 pixel sensor and by the needs of the experiment, to cover a FOV at the target range of 2 m. The parameters at our disposal are the geometry (sensor to sensor separation angle and sensor to target range, and hence to angular FOV and the IFOV), and the sensor location and LOS pointing measurement error. We accept a 0.5 pixel tracking accuracy as given.

There are many ways to approach this problem. We begin by addressing the 1 mm frame to frame accuracy requirement. For this, only the tracking accuracy matters, and equation (5) may be reduced to equation (9):

$$\sigma_{x_t} = rc_{x,\theta}\sigma_{\theta} = rc_{x,\theta}\sigma_{pix}IFOV \qquad (9)$$

Our 1 mm frame-to-frame target position requirement is $\sigma_x$, r is the sensor to target horizontal range, and $\sigma_\theta$ is our angular measurement error: tracking error in pixels ($\sigma_{pix}$) multiplied by the IFOV. We can use these to place a limit on $c_{x,\theta}$ and this in turn can be used to specify a minimum sensor to sensor separation angle. The IFOV is related to the sensor to target range r, the target plane FOV (d = 2 m), and the sensor pixel count ($N_x$ = 1000) by equation (10):

$$IFOV = 2\tan^{-1}\left(\frac{d}{2r}\right)\frac{180}{N_x \pi} \qquad (10)$$

Assuming that d/2r is sufficiently small that we ignore the difference between d/2r and $\tan^{-1}$(d/2r), we can insert this into equation (9) and solve for $c_{x,\theta}$, giving equation (11):

$$c_{x,\theta} = \frac{\sigma_x}{\sigma_{pix}}\frac{N_x}{d}\frac{\pi}{180} \qquad (11)$$

We observe that the sensor to target range has cancelled out. Inserting values for our pixel count, tracking accuracy, FOV coverage, and accuracy requirement, we obtain a value of $c_{x,\theta}$ = 0.017. Referring to Figure 3, this can only be achieved with a sensor-to-sensor separation angle of 90 degrees. Equation (11) also tells us that if we cannot arrange to have this ideal geometry, we must either increase our sensor pixel count, decrease our track error, or decrease our FOV coverage. Note that we could look up the value of $c_{x,\theta}$ for a separation angle of 90 degrees and then examine the trade-off between accuracy requirements for target location and tracking measurement accuracy, FOV coverage, or sensor pixel count.

Having established our separation angle, we now need to determine the sensor LOS accuracy and sensor location accuracy necessary to meet our absolute position requirement of 5 mm. We begin by once again re-writing equation (5), this time splitting out the tracking error (1 mm) and using equation (10). Our sensor LOS error (e.g. 1 pixel) is $\sigma_{LOS}$.

$$\sigma_{x_t} = \sqrt{c_{x,pos}^2\sigma_{pos}^2 + (1mm)^2 + c_{x,\theta}^2\left(\frac{180d}{\pi N_x}\right)^2\sigma_{LOS}^2} \qquad (12)$$

All of the numbers here are now known quantities except the sensor location error and the sensor LOS error. Looking up values for the error coefficients (Figure 3) at a separation angle of 90 degrees, equation (12) reduces to:

$$(5mm)^2 = \sigma_{pos}^2 + (1mm)^2 + (1.9mm/pixel)^2\sigma_{LOS}^2 \qquad (13)$$

This result can be used to partition measurement errors between the sensor LOS accuracy (in pixels) and the sensor location accuracy. If we assume that we can align our LOS to within 1 pixel, then we are left with $\sigma_{pos}$ = 4.5 mm for our sensor location error.

The sensor-to-target range has not been specified. It turns out that for low elevation angles, this is not important. This allows the test designer to adjust the sensor to target range to match the FOV of a given focal length lens to the FOV coverage requirement. Of course, as range is increased the baseline distance between sensors must be increased in order to maintain a constant separation angle.

## 5. SUMMARY

This paper has extended previous work by simplifying the working equations and providing simplified graphs of the error propagation coefficients for two-sensor, 3D triangulation. This serves to make the basic error estimation procedure more accessible and less error prone.

This work uses these results to show how to analyze the accuracy of a triangulation system typical of automotive crash test applications. For the typical test setup described, a tracking accuracy of 2 mm was predicted, with an absolute position accuracy of 6 mm. These results were compared with the accuracy expected from the more common single sensor approach in which a reference object in the imagery is used to calibrate target motion in a plane. The single camera scaling approach was predicted to give an accuracy of 1 mm. Increasing the sensor-to-sensor separation angle to 90° was found to improve the triangulation accuracy to 1 mm, matching but not exceeding that of the single sensor approach. The conclusion to be drawn from this is that while the triangulation approach offers significant advantages for studying non-planar motion, or for tracking targets for which no suitable calibration objects are present, this approach will not exceed the accuracy of a well designed single sensor system when studying planar target motion.

This paper also presented a methodology to work from a given accuracy requirement to a test setup design, again using the simplified error coefficient graphs developed at the beginning of this work. In particular, equation (11) relates frame to frame target location accuracy (essential for good velocity estimates) to target tracking accuracy (in pixels), sensor pixel count, target plane coverage, and the error propagation coefficient. This in turn allows one to determine the minimum sensor separation angle.

While this paper addresses the impact of measurement error in a triangulation system, it does not address how to make sensor location and LOS measurements or calibration. However, a basic discussion of some of the contributing error sources has also been provided.

## REFERENCES


1. "Image-based motion measurement: new technology, new applications", J.S. Waldon, Proc of the SPIE, **2513**, August 1994.
2. "Vehicle Real-time Attitude Estimation System (VRAES)", J.N. Sanders-Reed, Proc of the SPIE, **2739**, April 1996.
3. "Error propagation in multi-sensor 3D position estimation", J.N. Sanders-Reed, Optical Engineering, **40 (4)**, April, 2001.
4. "Algorithms for fully automated three-dimensional particle tracking velocimetry", Y.G. Guezennec, R.S. Brodkey, N. Trigui, J.C. Kent, Experiments in Fluids, **17**, 1994.
5. "Reconstruction of a 3-dimensional flow field from orthogonal views of seed track video images", A.A. Adamczyk, L. Rimain, Experiments in Fluids, **6**, 1988.


## CONTACT


Dr. Sanders-Reed is a Boeing Technical Fellow. He holds a Ph.D in physics from Case Western Reserve University and an MBA in high technology from Northeastern University. He may be contacted at Jack.Sanders-Reed@boeing.com.